Electronic Refrigeration at the Quantum Limit

Andrey V. Timofeev,[1, 2] Meri Helle,[1] Matthias Meschke,[1] Mikko Möttönen,[1, 3, 4] and Jukka P. Pekola[1]

[1]*Low Temperature Laboratory, Helsinki University of Technology, P.O. Box 3500, 02015 TKK, Finland*
[2]*Laboratory of Superconductivity, Institute of Solid State Physics, Chernogolovka, 142432 Russia*
[3]*Department of Applied Physics, Helsinki University of Technology, P.O. Box 5100, 02015 TKK, Finland*
[4]*Australian Research Council Centre of Excellence for Quantum Computer Technology, The University of New South Wales, Sydney 2052, Australia*

We demonstrate quantum limited electronic refrigeration of a metallic island in a low temperature micro-circuit. We show that matching the impedance of the circuit enables refrigeration at a distance, of about 50 μm in our case, through superconducting leads with a cooling power determined by the quantum of thermal conductance. In a reference sample with a mismatched circuit this effect is absent. Our results are consistent with the concept of electromagnetic heat transport. We observe and analyze the crossover between electromagnetic and quasiparticle heat flux in a superconductor.

PACS numbers:

The fundamental limit of heat transport via a single channel is governed by the quantum of thermal conductance [1]. This phenomenon was verified experimentally for phonons [2, 3], electrons [4], and photons [5]. In the experiment by Meschke *et al.* [5], the contribution of heat conductance by photons was relatively weak due to impedance mismatch in the employed electrical circuit and due to strong electron-phonon coupling. Here, we demonstrate the importance of matching the circuit to reach the full quantum of heat conductance. Our experiment allows for direct observation of heat transport at the limit of one quantum. We also observe and analyze how two parallel heat conduction mechanisms in a superconductor — by quasiparticles and by thermal photons — dominate in different temperature regimes.

As discovered in 1928 by Johnson and Nyquist [6, 7], a resistor R in an electric circuit at temperature T produces thermal voltage noise with power spectrum given by $4k_BTR$ per unit frequency bandwidth. Therefore, two resistors R_1 and R_2 at different temperatures T_1 and T_2 exchange energy in a circuit with a net heat flux between them: heat flows from hot to cold according to the second law of thermodynamics. The heat flux discussed here is electromagnetic in nature [8], and it can be written as [9]:

$$P_\nu = \int_0^\infty \frac{d\omega}{2\pi}\frac{4R_1R_2\hbar\omega}{|Z_t(\omega)|^2}\left(\frac{1}{e^{\hbar\omega/k_BT_2}-1}-\frac{1}{e^{\hbar\omega/k_BT_1}-1}\right). \tag{1}$$

Here, $Z_t(\omega)$ is the frequency $\omega/2\pi$ dependent total series impedance of the circuit. Whether the heat exchange in a circuit is classical (as in [6, 7]) or quantum limited depends fundamentally on temperature T and on the (linear) size of the circuit ℓ, or, more precisely, whether the electromagnetic noise, mediating the heat between the two resistors, is cut-off at the characteristic frequencies of the circuit $\omega_c = (RC)^{-1}$ or $\omega_c = R/L$, or at the thermal frequency $\omega_T = k_BT/\hbar$. Rough estimates of unavoidable stray capacitances C and series inductances L are given by $C \sim \epsilon\ell$ and $L \sim \mu\ell$, where ϵ is the permittivity and μ the permeability of the medium. For a macroscopic room temperature $T = 300$ K circuit of $\ell \sim 1$ mm size, the noise is cut-off at the circuit frequency, $\omega_c/\omega_T \sim 10^{-2} \ll 1$ for the resistance $R = 100\ \Omega$, which is of the same order as that in our experiment. In this case the noise and the heat flux are classical, originating from the equipartition law, where each degree of freedom carries an energy k_BT on the average [7]. Here, the magnitude of the heat flux does not follow any universal dependence, but it is determined by the detailed circuit topology and impedances. For a low temperature micro-circuit as in our experiment, with $T = 100$ mK and $\ell \sim 100$ μm, we are in the quantum limit: $\omega_c/\omega_T \sim 10^2 \gg 1$. In this case, the heat flux is governed by the equilibrium thermal distribution of electromagnetic radiation of the resistor and is limited by the universal quantum of thermal conductance $G_Q \equiv \pi k_B^2 T/6\hbar$. This electromagnetic heat conduction mechanism dominates in electronic nanostructures [9, 10, 11, 12] over electron-phonon and normal electronic heat conduction as the temperature approaches zero.

To observe quantum limited refrigeration and to demonstrate the significance of impedance matching, we have devised a circuit shown in Fig. 1a. Two gold-palladium ($Au_{0.75}Pd_{0.25}$) normal metal islands on an oxidized silicon substrate at a distance $\ell = 50$ μm are connected into a loop by aluminium superconducting lines. The aluminium and gold-palladium metals are in a direct contact to each other, without a tunnel barrier, whereby the contact resistance is small, $< 1\ \Omega$. Each island is 3 μm long, 0.2 μm wide and 20 nm thick (see Fig. 1b) and the measured resistance of each of them is $R \simeq 230$ Ω. Each island is also connected to four external aluminium superconducting leads through aluminium oxide tunnel barriers, which form four normal-metal - insulator - superconductor (NIS) tunnel junctions, with the area of 150×150 nm^2 and measured normal state resistance $R_T \simeq 19$ kΩ each. Different pairs of these junctions are used to perturb and to measure the electronic tempera-

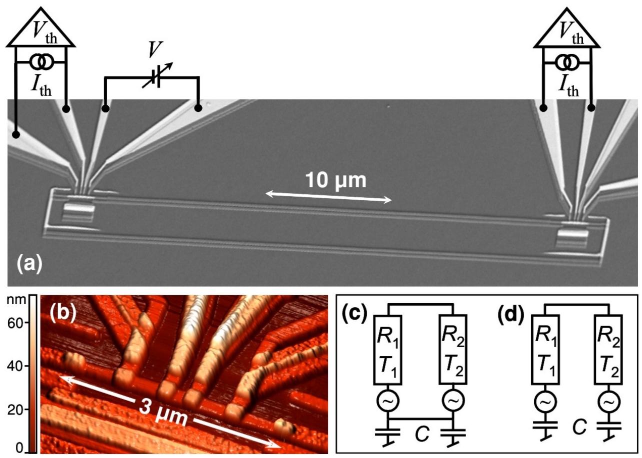

FIG. 1: (a) Electron micrograph of sample A. Two gold-palladium $Au_{0.75}Pd_{0.25}$ islands at a 50 μm distance are connected with aluminium superconducting lines into a loop to match the impedance between them and enable remote refrigeration. (b) Colored atomic force microscopy image of the island, connected at both ends directly to superconducting lines by metal-to-metal contacts. The four NIS junctions, contacting each island in the middle part, are used to perturb and to measure the island temperature. (c) Equivalent electrical circuit of the matched (sample A) and (d) the mismatched (sample B) structure.

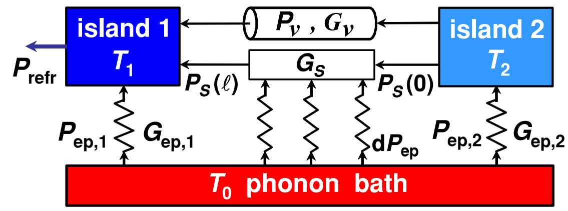

FIG. 2: The thermal model illustrates electromagnetic (P_ν, G_ν) and quasiparticle (P_s, G_s) heat conduction through the superconducting line between the two islands. The islands are thermally coupled to the phonon bath with the heat fluxes $P_{\text{ep},1}$ and $P_{\text{ep},2}$. The weak electron-phonon coupling of the superconducting line to the thermal bath is denoted by $\mathrm{d}P_{\text{ep}}$. The arrows show the direction of the heat flow for temperatures $T_1 < T_2 < T_0$.

ture of the islands, as detailed below. We have also fabricated and measured a similar reference sample, in which the two islands were connected only by a single superconducting aluminium line and were not enclosed into a loop. The two sample geometries in the experiment represent impedance matched (with loop geometry) and mismatched electrical circuits, which are schematically depicted in Figs. 1c and 1d, and which we denote sample A and sample B, respectively.

To show that impedance matching between the two islands is indeed vital for the observation of quantum limited refrigeration, we compare the rates P_ν in the matched and mismatched cases. For the matched sample A with $R_1 = R_2 = R$, $Z_t(\omega) = 2R$, we obtain from Eq. (1) the universal quantum heat flux: $P_\nu^{\text{A}} = \frac{\pi k_B^2}{12\hbar}(T_2^2 - T_1^2)$, which is $G_Q(T_2 - T_1)$ for a small temperature difference and presents the maximum heat flux possible for transmission through this electromagnetic channel. For the mismatched circuit with $R_1 = R_2 = R$, closed by the shunt capacitance $C/2 \sim 10$ fF which is determined mainly by the NIS junctions, we obtain $P_\nu^{\text{B}} \simeq \frac{\pi^3 k_B^2}{30\hbar}(T_2^2 - T_1^2)(k_B T R C/\hbar)^2$ for $T \approx T_1 \approx T_2$ at high circuit cut-off frequencies $\omega_c \gg \omega_T$. We find that $P_\nu^{\text{B}}/P_\nu^{\text{A}} \simeq \frac{2\pi^2}{5}(\omega_T/\omega_c)^2$; the electromagnetic power flow in the matched circuit is expected to be about $10^2 - 10^3$ times stronger as compared to that in the mismatched case at temperatures $0.3 - 0.1$ K relevant for the experiment.

The two samples were fabricated with the standard methods of electron beam lithography and shadow evaporation, and measured in a ^{3}He-^{4}He dilution refrigerator as follows. One pair of NIS junctions, the SINIS-refrigerator, connected to island 1, is DC-biased with voltage V to cool down the island by removing hot electrons from it into the superconducting leads through the tunnel barrier at voltages $eV < 2\Delta$ [13, 14, 15, 16]. Here $\Delta \simeq 200$ μeV is the superconducting energy gap of aluminium [17]. At higher bias voltages the island is heated up. To probe the island temperature T_1, the other pair of NIS junctions on the island is used as a thermometer by applying a small DC current I_{th} through it, and by measuring the corresponding temperature dependent voltage V_{th}. Another similar SINIS-thermometer probes the temperature T_2 of the second island. When the applied voltage V through the SINIS-refrigerator is zero, the measured voltage $V_{\text{th}}(V = 0)$ provides the thermometer calibration against the bath temperature T_0 when the cryostat temperature is varied in the range $50 - 500$ mK. The electronic temperature of the islands is then obtained from the fit of the dependence of T_0 on $V_{\text{th}}(V = 0)$. At $V = 0$ the electronic temperature coincides with the bath temperature down to $T_0 = 120$ mK. The thermometers have individual floating DC bias sources and do not cause excessive heating or cooling of the islands due to the low bias current, $I_{\text{th}} \simeq 0.001\Delta/eR_T$, used.

The thermal model that accounts for our set-up and observations is shown in Fig. 2. The resistors exchange energy at power P_ν through the electromagnetic channel, and, in parallel, at power P_s, due to quasiparticle heat conduction through the superconducting line. The latter contribution is significant at higher temperatures but diminishes exponentially towards low temperatures, $k_B T_0 \ll \Delta$ [18, 19]. We describe quantitatively quasiparticle heat flux with the heat diffusion equation

$$\frac{d}{dx}\left(-\kappa_s \frac{dT}{dx}\right) = \alpha(T_0)\Sigma_{\text{Al}}[T_0^5 - T^5(x)], \qquad (2)$$

assuming that the superconducting line has the temperature profile $T(x)$ with boundary conditions $T(0) = T_2$ and $T(\ell) = T_1$, where x is the coordinate along the line ($x = 0$ corresponds to the contact to island 2, $x = \ell$ to that to island 1). Factor $\alpha(T_0)$ determines the suppression of electron-phonon coupling in the superconducting line with respect to that in the normal metal state [18], and $\Sigma_{\rm Al} \simeq 0.3 \cdot 10^9$ WK^{-5}m^{-3} is a material constant for aluminium [16]. The heat flux $P_s(0) = -\kappa_s A T'(0)$ to island 1, and the heat flux $P_s(L) = -\kappa_s A T'(\ell)$ from island 2 are determined through temperature gradients $T'(0)$ and $T'(\ell)$ at the ends of the superconducting line with cross-sectional area $A = 200 \times 25$ nm^2. Here, $\kappa_s = \gamma(T_0)\kappa_n$ is the heat conductivity of the superconducting line [19], suppressed by a factor $\gamma(T_0) = \frac{3}{2\pi^2}\int_{\Delta(T_0)/k_B T_0}^{\infty} \frac{t^2 dt}{\cosh^2(t/2)}$ with respect to heat conductivity $\kappa_n = \ell L_0 T(x)/(R_\ell A)$ in the normal metal state determined by the Wiedemann-Franz law. Here, $L_0 \simeq 2.4 \cdot 10^{-8}$ WΩK^{-2} is the Lorenz number, and R_ℓ is the normal state resistance of the aluminium line; $R_\ell \simeq 138\ \Omega$ for sample A and $R_\ell \simeq 188\ \Omega$ for sample B. The electrons in each resistor of volume Ω_i exchange energy with the substrate, i.e., with the thermal bath at temperature T_0 via electron-phonon coupling at the rate $P_{{\rm ep},i} = \Sigma_{\rm AuPd}\Omega_i(T_0^5 - T_i^5)$ [20, 21, 22], where $\Sigma_{\rm AuPd} \simeq (2-4)\cdot 10^9$ WK^{-5}m^{-3} is obtained from the measurements. Island 1 can be SINIS-refrigerated (or heated) with the corresponding power $P_{\rm refr}$. We neglect phonon heat transport based on experimental results discussed below. The steady-state of the system is then described by the energy balance equations

$$\begin{aligned} P_{\rm refr} - P_\nu - P_s(\ell) - P_{\rm ep,1} &= 0 \\ P_\nu + P_s(0) - P_{\rm ep,2} &= 0. \end{aligned} \quad (3)$$

For the quantitative analysis of the remote refrigeration effect, we solve numerically Eq. (2) together with Eqs. (3) to obtain the relative temperature change of island 2 with respect to that of island 1, $\Delta T_2/\Delta T_1 \equiv (T_2 - T_0)/(T_1 - T_0)$. For small temperature differences, neglecting the electron-phonon coupling in the superconductor, we can linearize the different contributions in Eqs. (3) and obtain a particularly simple expression for $\Delta T_2/\Delta T_1$:

$$\frac{\Delta T_2}{\Delta T_1} = \frac{G_\nu + G_s}{G_\nu + G_s + G_{\rm ep,2}}. \quad (4)$$

Here, the photon coupling G_ν is expected to be equal to G_Q for the matched sample and for the mismatched sample it is suppressed by a large factor as discussed above. The electron-phonon conductance is given by $G_{\rm ep,2} = 5\Sigma_{\rm AuPd}\Omega_2 T_0^4$, and G_s denotes the ordinary heat conductance by quasiparticles in the superconducting line.

Upon sweeping the voltage V across the SINIS-refrigerator, both thermometers show cooling at $eV \lesssim 2\Delta$, indicating electronic refrigeration of both islands, see Figs. 3a and 3b. As expected, the SINIS refrigerating effect is maximal around the optimal bias voltage $eV \simeq 2\Delta$. The absolute temperature drops ΔT_1 and ΔT_2 of the two islands for the two samples are shown in Figs. 3c and 3d. In both cases, the direct SINIS refrigeration of island 1 is similar. In contrast, the refrigeration of the remote island is drastically different in the two samples. In sample A with the matched circuit, island 2 temperature tends to follow the temperature of the main island at low temperatures. In sample B with the mismatched circuit, the refrigeration of the remote island is suppressed at low temperatures. The corresponding

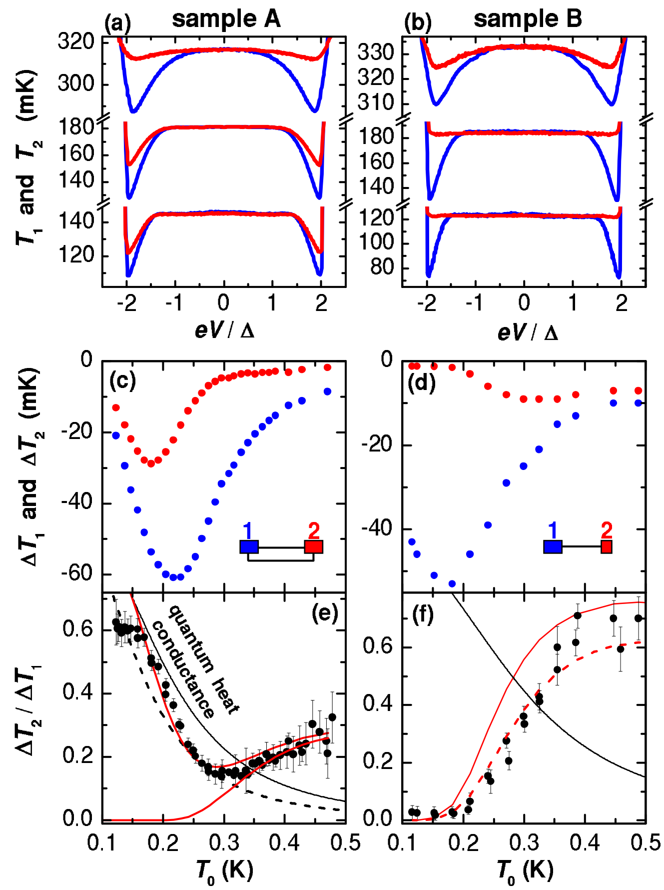

FIG. 3: Measured data of sample A (a, c, e) and sample B (b, d, f) and calculated results of the thermal model. (a), (b): Measured island temperatures T_1 (blue line) and T_2 (red line) vs. bias voltage V at a few bath temperatures T_0. (c), (d): Absolute temperature changes ΔT_1 (blue dots) and ΔT_2 (red dots) measured at bath temperatures 120 - 500 mK. (e), (f): Relative temperature changes obtained at 120 - 500 mK are shown by the black dots. The error bars show the standard deviation arising from the temperature calibration. (e), (f): The black lines are obtained from the linearized thermal model. The red lines are the results of the numerical thermal model. The solid lines are calculated with $\Sigma_{\rm AuPd} = 2\cdot 10^9$ WK^{-5}m^{-3} and the dashed lines with $\Sigma_{\rm AuPd} = 4 \cdot 10^9$ WK^{-5}m^{-3}.

relative temperature drops $\Delta T_2/\Delta T_1$ against T_0 at the optimum cooling bias voltage are plotted in Figs. 3e and 3f. For the matched sample $\Delta T_2/\Delta T_1$ has a minimum as a function of T_0 at about 300 mK; below this temperature it increases rapidly, as can be expected based on strong electromagnetic coupling. In the mismatched sample, $\Delta T_2/\Delta T_1$ vanishes towards lower temperatures, due to weak photonic coupling.

For the matched sample, the rise of $\Delta T_2/\Delta T_1$ at low temperatures in Fig. 3e is in agreement with the simple linearized thermal model: the data below 300 mK lie between the solid and dashed black lines, obtained from Eq. (4) assuming full quantum conductance $G_\nu = G_Q$ and vanishing quasiparticle conductance $G_s = 0$. Alternatively, the dashed black curve can be obtained from Eq. (4) with $G_\nu = 0.5G_Q$ and $\Sigma_{\rm AuPd} = 2 \cdot 10^9$ WK^{-5}m^{-3}, since only the photonic G_ν and the electron-phonon $G_{\rm ep,2}$ coupling contribute to the relative temperature drop $\Delta T_2/\Delta T_1$ when $G_s = 0$. At very low temperatures, the thermometer signal saturates. Based on these results we conclude that the matching in this sample is close to ideal and the refrigeration is limited by the quantum of thermal conductance. This effect is absent in the mismatched sample: for reference we show the black line in Fig. 3f with $G_\nu = G_Q$ and $G_s = 0$.

The quantitative behaviour of $\Delta T_2/\Delta T_1$ at high temperatures $T_0 \gtrsim 300$ mK is not universal and depends on sample parameters. In this temperature regime, the remote island of sample B is refrigerated more than that in sample A. This is because of stronger thermalization of sample A with larger island 2, and since there are, due to the deposition technique, extra normal (AuPd) shadows covering the vertical parts of the aluminium looped line (see Fig. 1a). In sample B, the normal shadow is not in contact with the superconducting line, which further enhances the quasiparticle mediated refrigeration. For Sample A, the data over the full temperature range are accounted for by the upper red line in Fig. 3e, obtained from the numerical analysis with $P_\nu = P_\nu^{\rm A}$ and $\Sigma_{\rm AuPd} = 2 \cdot 10^9$ WK^{-5}m^{-3}. To fit the data for sample A in the diffusion regime at temperatures above 300 mK, we added a fitting parameter $\alpha_N = 0.6$ to the factor α: $\alpha \to \alpha + \alpha_N$. The parameter α_N describes stronger thermalization of the superconducting line. The lower red line in Fig. 3e, calculated with $\alpha_N = 0.6$ and with no photonic heat exchange $P_\nu = 0$, shows quasiparticle contribution for comparison. For sample B, the numerically obtained red curves of quasiparticle conduction are shown in Fig. 3f. The dashed red curve shows good agreement with the data. The uncertainty in the quantitative comparison between the model and data arises from only approximately known parameters of electron-phonon coupling for gold-palladium and aluminium thin films.

In both samples, at voltages $eV > 2\Delta$, the probe islands are strongly heated due to hot quasiparticle injection in this regime. An additional thermometer, located near island 2, but not connected to it, was monitoring phonon temperature on the substrate. It showed negligibly weak temperature response as compared to the thermometers of islands 1 and 2. This supports our thermal model, which assumes that phonons provide a good thermal bath and that the observed heat exchange between the resistors occurs due to quasiparticles and electromagnetic coupling. This is a natural conclusion due to the very weak electron-phonon coupling at low temperatures.

In conclusion, we have demonstrated quantum limited refrigeration: the low temperature data show quantitative agreement with the thermal model assuming heat conduction determined by the quantum of thermal conductance. Furthermore, our observations and model account for residual heat conduction in a superconductor by quasiparticles. We suggest that even galvanically decoupled resistors can be refrigerated by the mechanism discussed. This could be an option for noise suppression purposes in sensitive quantum devices, e.g., by refrigerating shunt resistors [21] in SQUIDs (superconducting quantum interference devices).

We thank N. Chekurov for technical assistance in AFM imaging. This work is supported by the Academy of Finland, National Graduate School for Materials Physics, and the NanoSciERA project "NanoFridge" of the EU.

---

[1] J. B. Pendry, J. Phys. A. **16**, 2161 (1983).
[2] K. Schwab *et al.*, Nature **404**, 974 (2000).
[3] C. S. Yung, D. R. Schmidt, A. N. Cleland, Appl. Phys. Lett. **81**, 31 (2002).
[4] O. Chiatti *et al.*, Phys. Rev. Lett. **97**, 056601 (2006).
[5] M. Meschke, W. Guichard, J. P. Pekola, Nature **444**, 187 (2006).
[6] J. B. Johnson, Phys. Rev. **32**, 97 (1928).
[7] H. Nyquist, Phys. Rev. **32**, 110 (1928).
[8] There are generally other contributions of heat flux, which are often dominant, like that between the resistor and the phonon bath, i.e., the usual conduction to the surroundings, and electronic heat conduction along the wiring.
[9] D. R. Schmidt, R. J. Schoelkopf and A. N. Cleland, Phys. Rev. Lett. **93**, 045901 (2004).
[10] T. Ojanen and T. T. Heikkilä, Phys. Rev. B **76**, 073414 (2007).
[11] T. Ojanen and A. P. Jauho, Phys. Rev. Lett. **100**, 155902 (2008).
[12] D. Segal, Phys. Rev. Lett. **100**, 105901 (2008).
[13] M. Nahum, T. M. Eiles, J. M. Martinis, Appl. Phys. Lett. **65**, 3123 (1994).
[14] M. M. Leivo, J. P. Pekola, D. V. Averin, Appl. Phys. Lett. **68**, 1996 (1996).
[15] A. M. Clark *et al.*, Appl. Phys. Lett. **86**, 173508 (2005).
[16] F. Giazotto *et al.*, Rev. Mod. Phys. **78**, 217 (2006).
[17] The measured value of Δ is 200 ± 5 μeV for sample A and 210 ± 5 μeV for sample B.
[18] A. V. Timofeev *et al.*, Phys. Rev. Lett. **102**, 017003

(2009).
[19] J. Bardeen, G. Rickayzen, L. Tewordt, Phys. Rev. **113**, 982 (1959).
[20] M. L. Roukes *et al.*, Phys. Rev. Lett. **55**, 422 (1985).
[21] F. C. Wellstood, C. Urbina and J. Clarke, Phys. Rev. B **49**, 5942 (1994).
[22] The volume Ω_2 of island 2 for sample A is $1.2 \cdot 10^{-20}$ m^3 and for sample B it is $4.3 \cdot 10^{-21}$ m^3.